BIOSYSTEMS ENGINEERING 143 (2016) 108–118

Available online at www.sciencedirect.com

ScienceDirect

journal homepage: www.elsevier.com/locate/issn/15375110

Research paper

Diagnosis and detection of phosphorus nutrition level for *Solanum lycopersicum* based on electrical impedance spectroscopy

Li Meiqing [a], *Li Jinyang* [a,*], *Mao Hanping* [a], *Wu Yanyou* [a,b]

[a] *Key Laboratory of Modern Agricultural Equipment and Technology, Ministry of Education of the People's Republic of China, Institute of Agricultural Engineering, Jiangsu University, Zhenjiang 212013, PR China*

[b] *State Key Laboratory of Environmental Geochemistry, Institute of Geochemistry, Chinese Academy of Sciences, Guiyang 550002, PR China*

ARTICLE INFO

Article history:
Received 25 July 2015
Received in revised form
12 January 2016
Accepted 14 January 2016
Published online 8 February 2016

Keywords:
Solanum lycopersicum
Phosphorus nutrition level
Diagnosis and detection
Electrical impedance spectroscopy

Phosphorus (P) performs a key function in crop yield and quality. P deficiency frequently occurs in crop production and degrades crop yield and quality. Excessive P fertilisers cause environmental pollution and increase production cost. Therefore, diagnosis and detection of P content in plants are impending. Crop P monitoring methods have been developed to improve P fertiliser management, and most of these methods are based on leaf or canopy optical property measurements. However, sensitivity to environmental interference remains an important drawback. Electrical impedance has been applied to determine the physiological and nutritional status of plant tissue, but no studies related to plant P content have been reported. The objective of this article is to analyse how electrical impedance response of tomatoes is influenced by P nutrition status and explore the feasibility of P-deficiency detection by electrical impedance measurement. Five sets of tomato with different P source concentrations are used. Total P and electrical impedance spectra within the frequency range of 1 Hz–1 MHz are measured. The measured impedance data are analysed by using the modified model. The changes in equivalent parameters are analysed, the influence of moisture content on impedance measurement is discussed, and the characteristic frequency band is obtained. Then, we established the regression prediction model between total P and electrical impedance. High and positive correlation is observed between plant P content and impedance values at the obtained characteristic frequencies. Results suggest that electrical impedance can be applied to the detection and diagnosis of plant P nutrition status.

1. Introduction

Tomato is a principal greenhouse commercial crop in China, with a cultivated area of approximately 960 ha. Nitrogen (N), phosphorus (P), and potassium (K) constitute the major nutrition elements that are necessary for crop growth, crop yield, and quality (Kumar et al., 2015). It is easy for ratio imbalance and deficiency symptoms of N, P and K to appear in

* *Corresponding author*. Fax: +86 051188797338.
E-mail address: by0817136@163.com (L. Jinyang).
http://dx.doi.org/10.1016/j.biosystemseng.2016.01.005
1537-5110/

Nomenclature

C	capacitance (F)
CNLS	complex nonlinear least square
CPE	constant phase element
EIS	electrical impedance spectrum
EPI	electrode polarisation impedance
GPIB	general parallel interface bus
j	imaginary unit
K	potassium
N	nitrogen
P	phosphorus
PC	personal computer
PCA	principal component analysis
q	CPE exponent
r	correlation coefficient
R	resistance (Ω)
RMSE	root-mean-square error
SD	standard deviation
T	CPE coefficient
ω	angular frequency
x	independent variable
X	reactance (Ω)
Y	dependent variable
Z	impedance
$\|Z\|$	impedance magnitude (Ω)
θ	phase angle of impedance

Subscripts

e	extracellular
i	intracellular
m	cell membrane

the process of tomato growth and development. However, the deficiency and excess of NPK lead to important influences on crop and environmental pollution. Therefore, timely and accurate monitoring for NPK nutrition levels in tomato is of considerable significance to improve tomato NPK element management level and use efficiency. Moreover, monitoring can also conserve fertiliser and reduce excessive fertiliser pollution to the environment. The nutrition elements necessary for crop growth are provided by fertiliser application, and variable fertilisation is the ideal way to provide nutrition. However, nutrition detection and diagnosis is the first and most important problem in accurate variable fertilisation.

The visible symptoms which are caused by nutrient deficiency commonly destroy growth and metabolic balance in plants and thus lead to a change in crop internal structure. Morphological changes gradually appear when this kind of internal structure change develops to a significant extent. Once the symptoms can be seen, crops would have already suffered nutrient deficiency damage. The loss may still not be recovered even by fertiliser application in these circumstances. The rapid and accurate detection of plant nutrient status before evident symptoms appear is of considerable significance in guiding fertiliser application and maximising productivity. Among all nutrition detection methods, the chemical test method hardly meets the requirements of modern agricultural development but is still the traditional method of nutrition detection.

In recent years, rapid, real-time, on-line, and non-destructive detection is one of the research hotspots in the agricultural engineering field. In terms of rapid, real-time, and non-destructive detection of crop nutrients, research on nutrient detection and deficiency diagnosis methods in rice, corn, wheat, cotton, soybeans, cucumber, and tomato have been conducted through spectral analysis, machine vision technology, and multispectral and hyperspectral imaging technology. Although these works have verified that nutrition detection and diagnosis of crops could be realised by adopting feature information, such as texture, shape, colour, spectral reflectance, multispectral and hyperspectral image, most studies are confined to nitrogen detection and diagnosis. Research on rapid detection and diagnosis for P and K is more limited and currently is still in the exploratory stage (Wang et al., 2006). Moreover, non-invasive methods present limitations in terms of environmental sensitivity and confounding factors (i.e., soil condition, light intensity, canopy shape, and colour, etc.) (Rafael et al., 2014; Tomkiewicz and Piskier, 2012). Plant-tissue electrical properties are also modified by physical structure, chemical processes within, or the combination of both (Azzarello, Masi, Mancuso, 2012). Plant electrical impedance spectrum (EIS) is a method of measuring bioelectrical characteristics with a small amplitude sine wave voltage (or current) as the disturbance signal. Physiological and pathological information on biological tissues and organs can be provided in an extremely wide frequency range by the non-destructive determination of electrical impedance spectroscopy parameters, such as cell internal resistance and extracellular resistance, among others. Moreover, a comprehensive qualitative and quantitative analysis of the inner components of the composition and microstructure for the object can be conducted. Parameters of EIS can accurately reflect changes in the physical chemistry of biological tissue (Khaled, Castellano, Gazquez, García Salvador, & Manzano-Agugliaro, 2015). If we can monitor change in internal structure by using electrical impedance spectrum measurements on crops, early monitoring of their nutritional status can be implemented before the plants show obvious symptoms. In consequence, the early detection and diagnosis of P and K nutrition levels can be achieved.

Several researchers have reported methodologies for electrical impedance measurements to determine physiological status of plant tissues (Chi et al., 2012; Juansah et al., 2012). Potato tubers and carrot roots were analysed by using a double-shell model (Zhang and Willison, 1991). A Cole–Cole model was applied to evaluate the electrical impedance response of Scots pine needles (Zhang, Repo, Willison, Sutinen, 1995). Damaged tissue in bruised apples was detected (Jackson and Harker, 2000), and a relationship between electrical impedance and fruit biochemical properties (pH, sugar content, ripening) was determined (Liu, 2006). A willow root system was also assessed via electrical impedance measurements (Cao, Repo, Silvennoinen, Lehto,, & Pelkonen, 2011). To detect plant water status in tomato, He and collaborators developed a portable system (He et al., 2011). EIS was used for electrical characterization of fruits and vegetables (Khaled et al., 2015). However, few studies have focused on detecting nutrition status in plants. Greenham and collaborators studied electrical impedance measurements obtained

from phosphorus- and potassium-deficient *Trifolium subterraneum* plants (Greenham, Randall, Müller, 1982), and tomato plant stress caused by lack of nutrients was assessed (Tomkiewicz and Piskier, 2012).

As mentioned above, electrical impedance has been widely used to determine the physiological status of plant tissues and agricultural product quality due to the simplicity and effectiveness of the method. Furthermore, electrical impedance measurements are less sensitive to environmental variables and other factors in comparison with non-invasive methods that are used to determine crop physiological status. However, limited research on plant nutrition status detection has been conducted, and no studies have focused on analysing the effect of plant P status on electrical impedance. These research results provide a theoretical basis and some successful cases regarding the detection and diagnosis of tomato P nutrition levels by using EIS. However, a method of implementing the early-stage, rapid, and nondestructive detection of P by leaf impedance spectrum has yet to be established. Compared with other nutrition detection methods, such as spectroscopy and image analysis, the advantage of the nutrition detection method presented in this paper is that it should be less sensitive to environmental variables and other factors. The objective of this article is to analyse how the electrical impedance response of tomatoes is influenced by their P nutrition status and explore the feasibility of P deficiency detection by EIS.

2. Materials and methods

Experiments were carried out in the Venlo greenhouse and the laboratory of the Agricultural Engineering Institute of Jiangsu University in China.

2.1. Sample preparation

The cultivar Hybrid "908" (Long march seed co., LTD, Shanghai, China) of tomato (*Solanum lycopersicum*) was used as it is widely planted in China and has big fruits. Tomato seedlings were grown in the Venlo greenhouse and cultivated in nutrient solution. The nutrient solution followed the Yamazaki formula (Yu and Zhao, 2005). Same-sized seedlings were selected for experiments. Samples with different P nutrition levels were cultivated by using nutrient solution with five different P element contents, in which the P content was 25%, 50%, 75%, 100% and 125% of the Yamazaki formula, marked as P25, P50, P75, P100, and P125, respectively (Table 1).

P125 is obtained by adding NaH_2PO_4 with corresponding quotients on the basis of the standard Yamazaki solution. The tomato seedlings were watered by standard solution at early growth stages and by nutrient solution with five different P contents after 3 to 4 true leaves had grown, with four replicates per treatment. P absorption of plants is greatest at the seedling stage (the stage before flowering stage), and about 90% of the uptake in the whole growth period. P deficiency in the seedling stage affects flower bud differentiation. Therefore, this study mainly focuses on the P absorption of plants at the seedling stage.

Table 1 – Chemical composition (in mg L^{-1}) of nutrient solutions with various P concentrations based on Yamazaki solution for tomato.

	P125	P100	P75	P50	P25
$Ca(NO_3)_2 \cdot 4H_2O$	354	354	354	354	354
KNO_3	404	404	404	404	404
$(NH_4)H_2PO_4$	77	77	58	39	19
$MgSO_4 \cdot 7H_2O$	246	246	246	246	246
$(NH_4)_2CO_3$	0	0	10	20	30
NaH_2PO_4	20	0	0	0	0
Na2Fe-EDTA	25	25	25	25	25
H_3BO_3	2.13	2.13	2.13	2.13	2.13
$MnSO_4 \cdot 4H_2O$	2.86	2.86	2.86	2.86	2.86
$Zn\ SO_4 \cdot 7H_2O$	0.22	0.22	0.22	0.22	0.22
$Cu\ SO_4 \cdot 5H_2O$	0.08	0.08	0.08	0.08	0.08
$(NH_4)_6Mo_7O_2 \cdot 4H_2O$	0.22	0.22	0.22	0.22	0.22

2.2. Electrical impedance measurement

Impedance measurement was carried out with a Solartron 1260A Impedance/Gain-Phase Analyzer (Solartron Analytical, England, UK). The impedance analyser that was employed in this study uses digital correlation techniques for measurement in the frequency range of 10 μHz–32 MHz. The basic accuracy is 0.1% for magnitude and 0.1° for phase measurements. This instrument allows both two-terminal and four-terminal measurements. The combination of the impedance analyser and the Solartron 1294 impedance interface offers high accuracy, repeatability, and versatility, and it has been extensively used for bio-impedance measurements on live subjects, electro-analytical systems, characterisation of thin films and coatings, biotechnology research, and food freshness investigations, among others (Bao, Davis, & Schmukler, 1992; Hinton & Sayers, 1998; Jorcin, Orazem., Pebere, & Tribollet, 2006). The schematic for the measurement system is shown in Fig. 1, and Fig. 2 shows the experimental device for electrical impedance measurement.

For impedance measurements, we used a 100 mV generator voltage and scanned 91 spot frequencies (logarithmic frequency intervals) between 1 Hz and 1 MHz. The four-terminal technique is a highly efficient method that largely minimises the EPI (electrode polarization impedance) problem. Therefore, the four-terminal configuration was used in this study. Four stainless needle electrodes with 1.0 mm diameter, 12 mm length, and 10 mm clearance were inserted into tomato leaves. The electrodes were connected to the impedance analyser with coaxial cables by means of the four-terminal pair configuration. The AC signal was injected into the sample through two current stimulus terminals from the 1294 impedance interface (GenHi and GenLo), and voltage measurements were made at another pair of terminals from the interface (VHi and VLo). The samples were divided into two groups, namely, the calibration sample group for impedance measurements and the validation sample group for testing leaf P and moisture content.

The online impedance measurements of disease-free leaves from five different treatments at were conducted every two days, and each sample was replicated five times. The 7th tomato leaf was selected, and the middle part of each

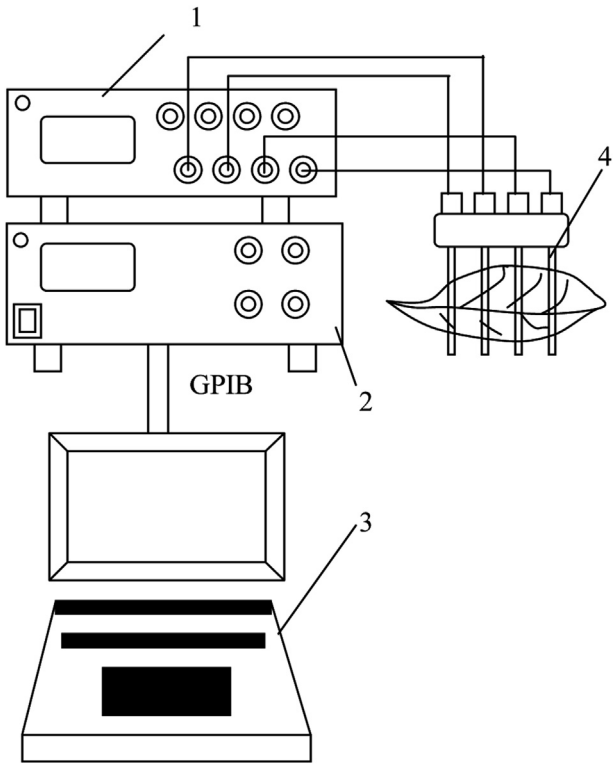

Fig. 1 – Schematic illustration for the measurement system of tomato leaves by four electrodes. 1-1294 Impedance Interface; 2-1260A Impedance/Gain-Phase Analyzer; 3-PC; 4-electrode.

blade away from the main vein was chosen as the test area. The tested area was quickly cleaned using a tissue prior to impedance measurement. The average value of the five replications was used in the analysis of results. The leaves from different treatments were picked and placed in polythene seal bags with labels immediately after electrical impedance measurement. The plucked leaves were then sent to the laboratory, and P content was determined by UV–vis spectrophotometry (Varian Inc., Palo Alto, USA; Model Gary 100).

The data were automatically transmitted from impedance analyser to a personal computer (PC) through a GPIB interface. Magnitude $|Z|$ and phase angle θ were measured directly from readings. All experiments were conducted inside a Faraday cage to isolate samples from electrical noise, particularly the line frequency of 50 Hz.

2.3. Models and curve-fitting

The determination of EIS characteristics can penetrate the biological material and comprehensively reflect changes in internal structure and composition of organisms. EIS generally utilises the electrical equivalent circuits of materials to characterise the experimental frequency response of impedance. The physical properties of the materials can be quantified by monitoring the changes in parameters of the equivalent circuit.

The resistance R (Ω) and reactance X (Ω) were calculated from Eqs. (1) and (2):

$$R = |Z|\cos\theta \quad (1)$$

$$X = |Z|\sin\theta \quad (2)$$

The relationships between the R and X of the complex impedance are shown by a Cole–Cole plot. Figure 3 shows four equivalent circuit models for biological tissues.

For biological tissue, the Cole–Cole plot was described as a circular arc (Cole, 1932). The Hayden model (Hayden et al., 1969) for plant tissues, which is shown in Fig. 3(a), considers the intracellular resistance R_i, extracellular resistance R_e, and the capacitance and resistance of the cell membrane, C_m and R_m. We can assume that the membrane resistance R_m can be ignored because the value of R_m is considerably larger than those of other parameters. Thus, the Hayden model can be expressed as the simplified Hayden model (Fig. 3(b)) (Wu, Ogawa, & Tagawa, 2008; Zhang and Willison, 1992). This model represents the structure of one cell and describes an exact semicircle in a Cole–Cole plot. However, tissues composed of numerous cells can produce a time constant distribution such that the Cole–Cole plot is described as a semi-ellipse. To model this semi-ellipse, we used a constant phase element (CPE) (Zoltowski, 1998) instead of C_m (Fig. 3(c)). As the use of a CPE can facilitate accurate model fitting to the equivalent circuit, CPE has been used in numerous studies (Itagaki, Taya, Watanabe, & Noda, 2002; Ricciardi, Ruiz-

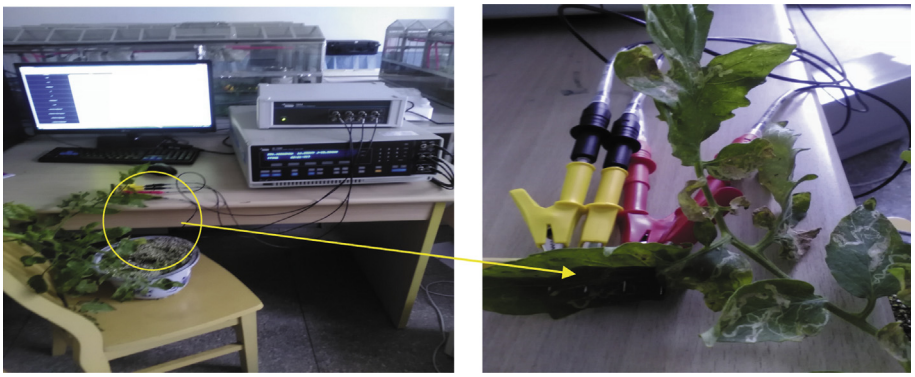

Fig. 2 – Experimental device for electrical impedance measurement of tomato leaf.

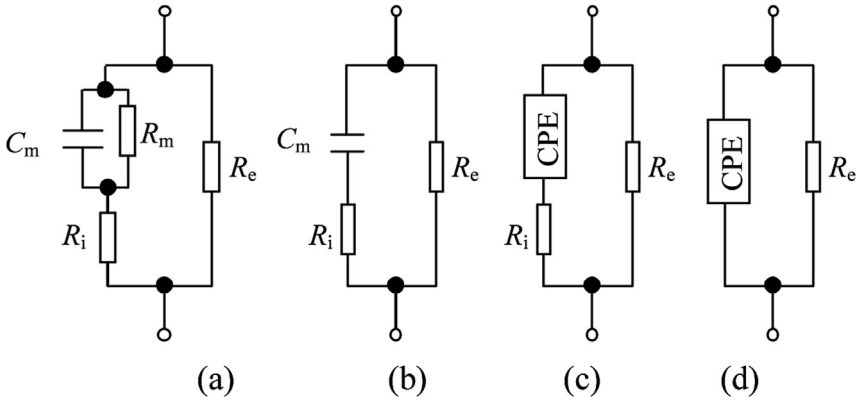

Fig. 3 – Equivalent circuit models for biological tissues. (a) Hayden model (b), Simplified Hayden model, (c) Modified model, (d) R_e-CPE parallel circuit model. R_m: intracellular resistance of cell membrane, C_m: capacitance of cell membrane, R_i: intracellular resistance and R_e: extracellular resistance.

Morales, & Nunez, 2009; Skale, Dolecek, & Slemnik, 2007). The expression of CPE can be described as

$$Z_{CPE} = \frac{1}{j\omega^q T} = \frac{1}{\omega^q T}\cos\left(\frac{q\pi}{2}\right) - j\frac{1}{\omega^q T}\sin\left(\frac{q\pi}{2}\right) \quad (3)$$

where j is the imaginary unit, ω is the angular frequency, T is the CPE coefficient, and q is a CPE exponent in the range of 0–1 that describes the time constant distribution in the system. Upon analysis and observation of impedance data, the shape of the Cole–Cole plot is an exact semi-ellipse. Hence, the modified model was applied for the tomato tissue samples in this study. The complex impedance of the modified model can be described (Yasumasa, Koichi, Naoto, 2014) by:

$$Z = \frac{R_e\{1+\omega^q T[(2R_i+R_e)\cdot\cos(q\pi/2)+\omega^q T\ R_i(R_e+R_i)]\}}{\omega^q T(R_e+R_i)^2+2\omega^q T(R_e+R_i)\cdot\cos(q\pi/2+1)} \\ j\cdot\frac{\omega^q T\ R_e^2\cdot\sin(q\pi/2)}{\omega^q T(R_e+R_i)^2+2\omega^q T(R_e+R_i)\cdot\cos(q\pi/2)+1} \quad (4)$$

Equivalent parameters were estimated using complex nonlinear least square (CNLS) curve-fitting (Macdonald, 1992). In the CNLS fitting, the sum of the squares of real and imaginary residuals was minimised.

The unit of T varies with the values of q. Therefore, q values must be fixed to accurately analyse the capacitive components of the cell membrane. T can be expressed as apparent C by using Eq. (5) (Hsu and Mansfeld, 2001). Notably, we assume that the relaxation angular frequency (the angular frequency at which the imaginary part of the impedance Z is minimum) keeps the same.

$$C = T\omega_m^{q-1} \quad (5)$$

where ω_m is the relaxation angular frequency. The ω_m of the modified model can be calculated using the following equation:

$$\omega_m = \frac{1}{T(R_e+R_i)^{-q}} \quad (6)$$

From Eqs. (4) and (5), we can obtain the following expression,

$$C_m = T^{\frac{1}{q}}(R_e+R_i)^{\frac{1-q}{q}} \quad (7)$$

In this study, C_m is defined as the cell membrane capacitance and is calculated by substituting the values of each parameter in the modified model into Eq. (7).

To carry out qualitative analysis for impedance value differences resulting from different P treatments, we conducted principal component analysis (PCA) for impedance. The matrix was built by using P contents and 91 impedance values with the range from 1 Hz to 1 MHz, from 20 samples (5 treatments, 4 repeats). The regression model of phosphorus content was developed on the basis of stepwise regression analysis for impedance value differences resulting from different P treatments.

In order to evaluate the validity of the built regression model of phosphorus content, the calibration and validation were conducted. The detailed steps are as follows: 1) impedance measurements of leaves from samples with different P contents were carried out at sensitive frequency (the detailed determination ways as shown in Section 3.4); 2) leaves under different treatments were picked and immediately placed in polythene seal bags with labels immediately after electrical impedance measurement; 3) plucked leaves are sent to the laboratory, and P content is determined; 4) prediction values were calculated using the regression model of phosphorus content, and the model was evaluated by practical measurement values and model prediction values.

3. Result and discussion

3.1. *Behaviour of the impedance characteristics for different P nutrition level*

Figure 4 shows the changes in P content of five different treatments, P25, P50, P75, P100 and P125, and Eq. (8) describes the relationship between P_ source (the percentage of total P supplied by standard Yamazaki solution) and plant total P-content (%):

$$Total\_P = 0.0022 \times P\_source + 0.2339 \quad (8)$$

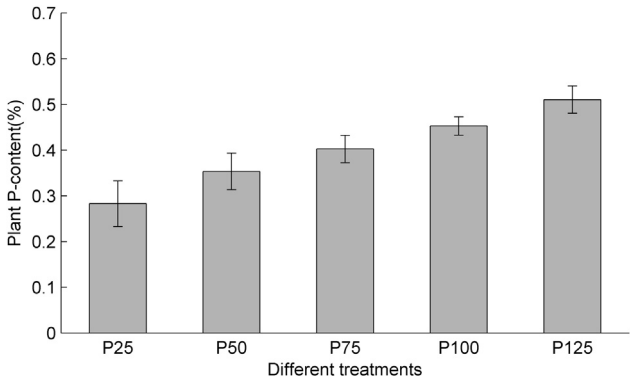

Fig. 4 – P-content averages (n = 5) related to the percentage of phosphorus.

From Fig. 4, it is clear that P_ source and plant total P-content are highly correlated and the P contents of samples from five different treatments are obviously different, and these samples can be applied in subsequent analysis.

Z-view software was used to perform curve fitting and data analysis was conducted in Matlab 7.1. The impedance of the samples plotted with respect to frequency is shown in Fig. 5. From Fig. 5, it is clear that the impedance declined noticeably as the frequency increased, and this phenomenon is called dispersion. In the low-frequency region, given the high electrical capacity of cell membranes, current flows through the extracellular fluid, which exhibits a relatively high resistance. However, in the high-frequency region, impedance decreases greatly because the current is able to flow through the intracellular fluid, which possesses a relatively low resistance. This phenomenon, which results from cell structures in biological tissue, is called β dispersion (Pethig and Kell, 1987). The modulus of impedance in lower frequency ranges decreases as K deficiency increases (Fig. 5). This result indicates a decrease in extracellular resistance. Phosphorus is an important constituent of the phospholipid bilayer of cell membrane and P deficiency leads to a decline in cell membrane area.

Resistance and the absolute value of reactance were plotted in the Nyquist plot (Fig. 6). The curve displays a semi-elliptical arc, with its centre below the X-axis. The curve can be described by the modified model shown in Fig. 3(c). However, we can see from Fig. 6 that the shape of the Nyquist Plot for P100 was obviously different from the other five measurements. P deficiency or excess had an effect on the physiological characteristics and cell structures of the plants and thus influenced the impedance characteristics of the samples. The specific mechanisms can be investigated by observing the variations in cell structure using a high-resolution microscope and by studying the effect of metabolites, such as protein, chlorophyll, soluble sugar, and cellulose, on impedance characteristics. Moreover, the measurement values from different treatments were close at low or high frequencies. This finding can be interpreted as follows: at high frequencies, the capacity of cell membrane C_m can be ignored because the value of C_m is considerably smaller than that of other parameters. Impedance mainly depends on extracellular and intracellular resistances. Though P deficiency or excess had an

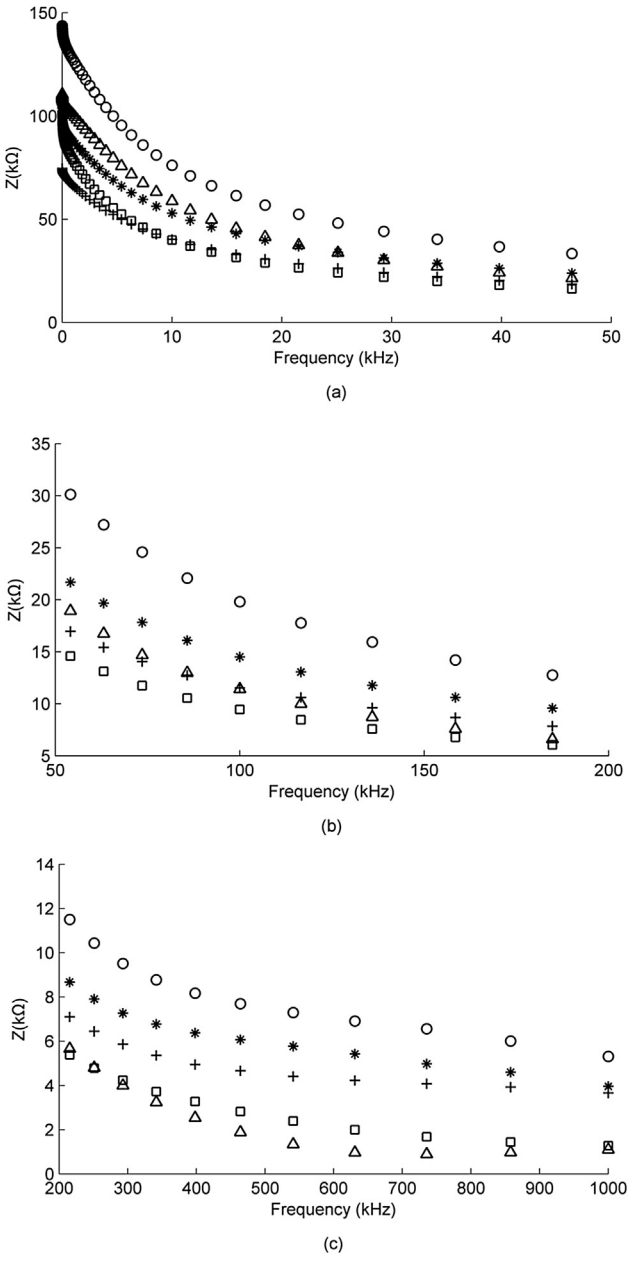

Fig. 5 – Changes in the impedance spectra of the tomato leaf at different phosphorus content plotted with respect to frequency. ○-P25; *-P50; +-P75; □-P100; Δ-P125.

evident effect on cell membrane C_m, this can be ignored at high frequencies, and thus measurement values from different treatments are close.

However, in low frequency regions, electrical current flows only through the extracellular fluid, which has a relatively high resistance. This finding is due to the high electric capacitance of cell membranes. The impedance mainly depends on extracellular resistance, and thus measurement values from different treatments are also close.

To quantify the variations in the impedance characteristics shown in Figs. 5 and 6, we conducted equivalent circuit analysis. To verify the validity of model fitting, we fitted the

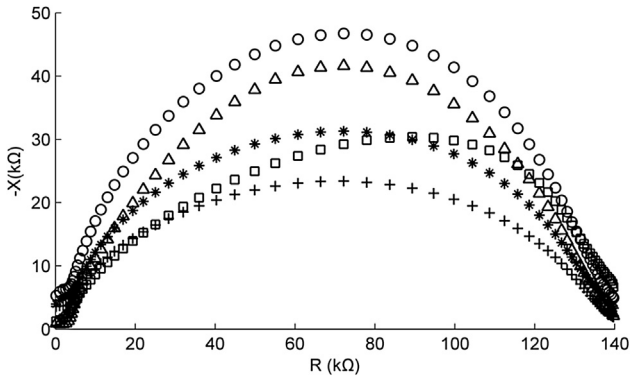

Fig. 6 – Changes in the Cole–Cole plot of the tomato leaf at different phosphorus content.

established model to experimental impedance values and evaluated the fitting accuracies. Figure 7 shows the approximation results of the models and experimental results of tomato leaf at a P content of 0.282%. The modified model presents high fit accuracy for both R and X, with corresponding R_R^2, R_X^2, and SD of 0.990, 0.995, and 40 Ω, respectively. R_R^2, R_X^2, and SD can be calculated from the following expressions:

$$R_R^2 = 1 - \frac{\sum_i \left(R_i - \widehat{R}_i\right)^2}{\sum_i \left(R_i - \overline{R}\right)^2} \tag{9}$$

$$R_X^2 = 1 - \frac{\sum_i \left(X_i - \widehat{X}_i\right)^2}{\sum_i \left(X_i - \overline{X}\right)^2} \tag{10}$$

$$SD = \sqrt{\frac{1}{N}\sum_i \left\{\left(X_i - \widehat{X}_i\right)^2 + \left(R_i - \widehat{R}_i\right)^2\right\}} \tag{11}$$

where N represents the number of measurement points, $\widehat{R}_i$ and $\widehat{X}_i$ denote the approximated values of R and X, and $\overline{R}$ and $\overline{X}$ are the mean values of R and X.

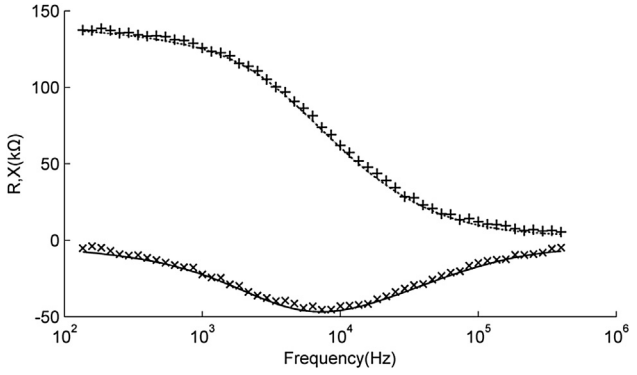

Fig. 7 – Approximation results of the model and experimental results of tomato leaf at P-content of 0.282%. +-Measured R; ×-Measured X; — -Calculated R; — -Calculated X.

By introducing CPE into the model, the phase angles of C_m were changed flexibly. Thus, the modified model properly describes the impedance characteristics of inhomogeneous tissues of the samples. This result was also demonstrated by Yasumasa et al. (2014). From the above analysis, the validity of the modified model was confirmed.

The modified model (in Fig. 3(c)) was used to analyse the impedance spectra of samples with different P content. The solid lines (in Fig. 7) represent the approximated values. The experimental data shows a good fit with the approximations. The values of R_R^2 for each sample were within the range of 0.944–0.993, and the values of R_X^2 were within the range of 0.934–0.995. The ratio of the standard deviation and average values (variation coefficient) were smaller than 0.866 for measured R, 0.912 for calculated R, 1.064 for measured X, and 0.972 for calculated X.

As shown in Fig. 8, variables R_i and R_e remained virtually constant when P content was larger than 0.45%. At P content below 0.45%, the capacitance of the cell membrane decreased as P content declined markedly. At P content of less than 0.32%, the decline in membrane capacitance is marked. Phosphorus is an important element of phospholipid molecules, and phosphorus deficiency affects the structure and function of the chloroplast membrane. Photosynthesis is significantly hampered when crops are phosphorus-deficient because phosphorus performs an important function in maintaining chloroplast structure and function. Therefore, we suspect that the decline in cell membrane capacitance occurs when P content is low, and cell membrane was damaged in P content less than 0.32%.

In normal cells, intracellular fluid with a relatively high concentration of electrolytes and extracellular fluid with low concentration are divided by the cell membrane (Yasumasa et al., 2014). The present results can be explained by assuming that the cell membrane of the sample was damaged by P deficiency and that intracellular fluid has leaked from the inside of the cells to the outside. The observation that the values of R_e and R_i were approaching each other as the extent of P deficiency increases supports this assumption.

From the above results, the ratio of R_e to R_i could be an index of cell health. The relationship between leaf phosphorus content and the ratio of R_e to R_i under different treatments is shown in Fig. 9. The ratio of R_e and R_i takes a value greater than 1, and the value decreases as cell injury becomes greater. The initial value of the ratio of R_e and R_i was approximately 335 and decreased with the extent of phosphorus deficiency extent. Faster changes in the ratio of R_e and R_i, which occurred at P content below 0.45%, suggest that the phosphorus deficiency influenced cell membranes.

In the region where P content is less than 0.32% (Fig. 8), the values of C_m are small, and the values of R_e sharply increase. These results can be explained if the cell membrane was seriously disrupted and that the noticeable change in R_e is mainly attributable to the P content deficiency.

3.2. *Relationship between impedance and moisture content*

Large amounts of water and metal ions are present in plants. The large content of moisture and metal ions inside tomato

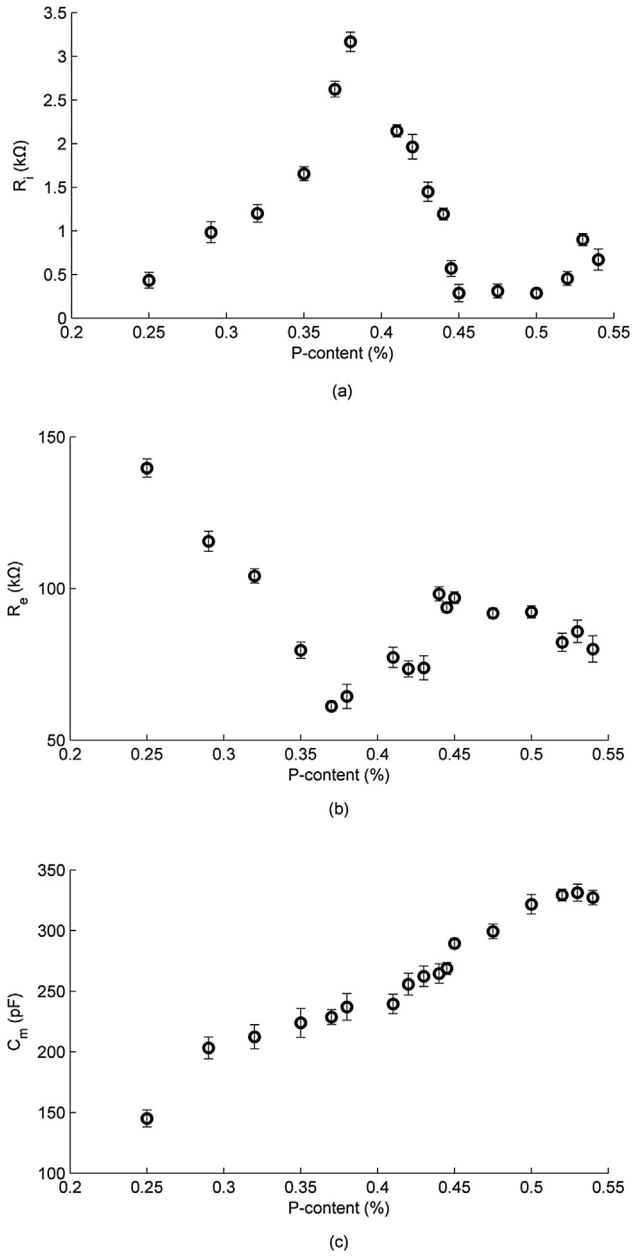

Fig. 8 – Relationship between phosphorus content and the equivalent circuit parameters. C_m: capacitance of cell membrane, R_i: intracellular resistance and R_e: extracellular resistance.

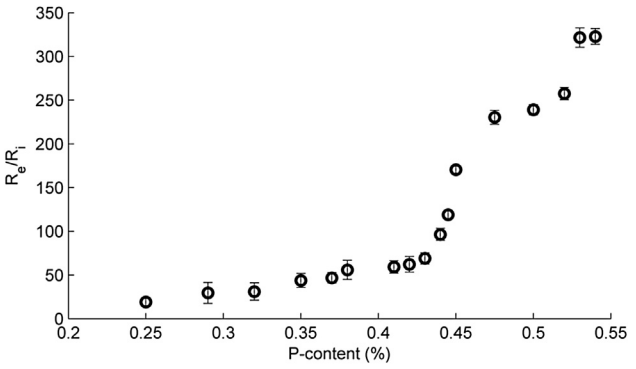

Fig. 9 – Relationship between phosphorus content and R_e/R_i

leaves allows the leaves to act as good electrical conductors. The variation in moisture content leads to changes in electrical conductivity and electrical impedance. The impedance was affected by the moisture content (Mizukami, Sawai, Yamaguchi, 2006; Yasumasa et al., 2014). To improve the diagnosis accuracy of P nutrition status in this study, we investigated the effect of moisture content on impedance measurement. To obtain the samples with different moisture contents, we conducted the following procedures. First, fresh leaves are picked, and the weight of each sample was recorded with a digital scale with a 0.01 g graduation immediately after electrical impedance measurement. Then, samples are placed in a thermostatic chamber and hot-air dried at 50 °C for 30 min. After every 30 min, the samples are taken out and weighed, and impedance measurement is repeated when sample temperature is close to room temperature. Finally, the samples are placed in a thermostatic chamber and hot-air dried at 105 °C for 12 h, the final weight of samples is acquired, and the moisture contents for the different stages are calculated. Figure 10 shows the changes in the Cole–Cole plot of samples with different moisture contents.

The semi-ellipse was considerably enlarged as the moisture content declined, and the impedance arc characteristic disappears when moisture content was less than 25%. The rapid increase in impedance can be explained by further moisture loss reducing the total amount of current paths. As a result, the activities of free ions are limited, and impedance increases.

Alternatively, the influence of fibre becomes apparent when moisture content is reduced to a certain level (as illustrated by 25% in this case). Tomato leaves represent a dielectric characteristic because of the woody characteristics of fibre. Therefore, the tested electrical signal mainly originates from fibre. Thus, the overall impedance magnitude jumped to a relatively high value. This finding is in good agreement with the phenomenon in potato during late drying, as suggested by Yasumasa et al. (2014). The above results indicate that moisture content noticeably affects the impedance values of tomato leaves. In this study, however, given that the moisture content of measured leaves are between 86.07% and 89.65%, the effect of moisture content on impedance values is not significant. Thus, this effect is negligible in subsequent analyses in this study. However, this effect of moisture content on impedance values must be taken into account if the moisture content changes within a wide range.

3.3. *Principal component analysis for tomato leaf impedance*

The score plot obtained from PC1 and PC2 for different treatments is shown in Fig. 11. The cumulative contribution rate of PC1 and PC2 exceeds 96%, reflecting the original information of multi-dimensional data indicators. Thus, the 91 impedance

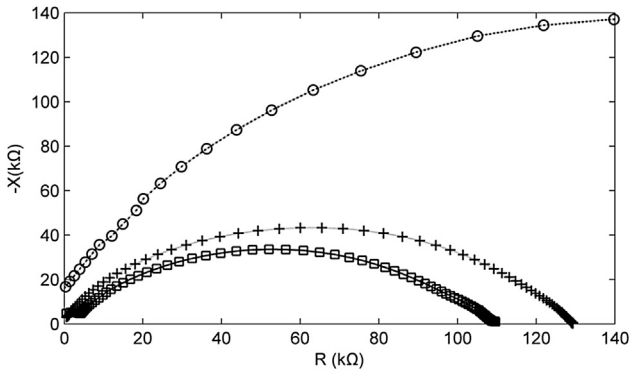

Fig. 10 – Cole–Cole plot of the samples with different moisture content. □-86%; +-54%; ○-25%.

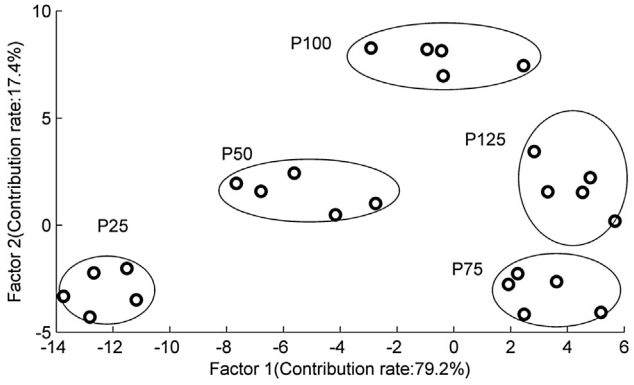

Fig. 11 – Scores plot obtained from PC1 and PC2 for different treatments.

values can be characterised by these two principal components, which covariance between these two principal components is equal zero. We can intuitively see from Fig. 11 that samples under different P treatments were dispersed in five different zones. This finding indicates that the impedance measurement method may be useful for qualitative discrimination of P nutrition status.

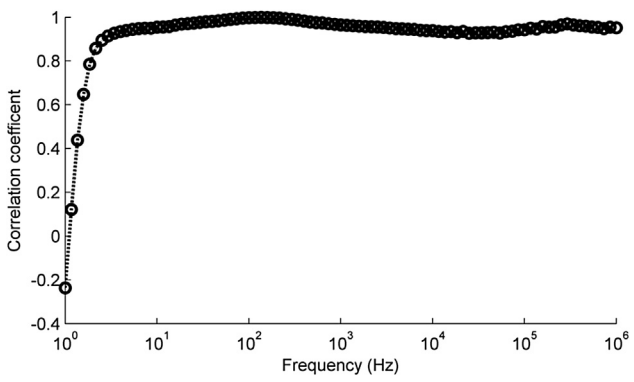

Fig. 12 – Correlation curves of tomato leaf impedance value and phosphorus content.

3.4. *Stepwise regression model based on leaf impedance and P mass fraction*

The positive correlation between leaf impedance values and P mass fractions is evident (Fig. 12), and significant correlation is present when the frequency is greater than 2.154 Hz. The correlation coefficient exceeds 0.85 in the frequency range between 2.154 kHz and 1 MHz. Therefore, to estimate and predict the P content in tomato leaves, we established a stepwise regression model for 20 leaf samples by selecting the modulus of impedance at 86 frequency points ranging between 2.154 kHz and 1 MHz as independent variable x and P mass fractions as dependent variable Y. Experimental samples were divided into two groups for the development of the stepwise regression model. The first group of samples was used for the establishment of the regression model and utilised 20 samples. The second group consisted of 14 samples and was used to validate the regression model. Statistical treatment of the data was performed using the SPSS software. The regression model of phosphorus content can be described in the following expression,

$$Y = 2.791 \ln(x_{61.96kHz}) - 29.119 \quad (12)$$

where Y is P mass fraction,% and $x_{61.96\ kHz}$ is the impedance modulus at 61.96 kHz, Ω.

Good coefficient of determination ($R^2 = 0.966$) and root mean square error ($RMSE = 0.1390$) were obtained during the calibration process.

In order to verify the validity of the built model as shown in Equation (12), the P content of the validation sample set was then predicted using the established model. Good predictions were obtained ($R^2 = 0.864$ and $RMSE = 14.573$). From these results, we can see that the obtained model exhibits excellent prediction performance and select 61.96 kHz as the sensitive frequency of P mass fractions is feasible. This result lays the foundation for developing an impedance analyser of plant P nutrition level. Predicted vs. measured values of P levels in tomato leaves for the validation set are shown in Fig. 13. A simple visual inspection of the narrow spread of experimental points along the straight line (reference line 1:1) in the figure shows that the predicted P contents are very accurate. This excellent prediction is confirmed by the slope of the straight line fit (not shown) of 0.94 and the offset (0.02%).

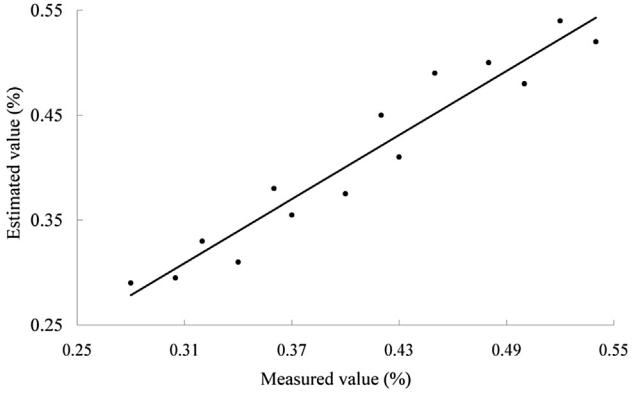

Fig. 13 – Estimated vs. Measured values of P levels in tomato leaves, and the 1:1 line.

4. Conclusion

We investigated the impedance characteristic of tomato leaves of plants fed with solutions of different P concentrations, to evaluate how electrical impedance response of tomatoes is influenced by P nutrition status and explore the feasibility of detecting P deficiency by EIS. The modified model was selected to describe the impedance frequency characteristics. The equivalent circuit analysis suggests that cell membranes were damaged by P deficiency and that intracellular fluid leaked out of cells. Results of principal component analysis (PCA) for impedance suggest that EIS can accurately discriminate between tomatoes with different P content. From the established stepwise regression model, high correlation between P content and the impedance values at sensitive frequencies was found. The potential of EIS as a method for evaluating the physiological status of biological cells was demonstrated. However the influence of other factors, such as diseases, other nutrients, and physiological variables in electrical impedance measurements should be assessed prior to further development of this approach for practical use.

Acknowledgements

A Project Funded by Key Projects in the National Science & Technology Pillar Program during the twelfth Five-year Plan Period (2014BAD08B03), Jiangsu Postdoctoral Science Foundation (1402076B), Jiangsu University Natural Science Instruction Plan Project (13JDG077) and the Priority Academic Program Development of Jiangsu Higher Education Institutions (Jiangsu fiscal education 2014-37).

REFERENCES

Azzarello, E., Masi, E., & Mancuso, S. (2012). .Electrochemical impedance spectroscopy. In *Plant electrophysiology. Germany: Heidelberg* (pp. 205–223).

Bao, J. Z., Davis, C. C., & Schmukler, R. E. (1992). Frequency domain impedance measurements of erythrocytes. *Biophysical Journal, 61*, 1427–1434.

Cao, Y., Repo, T., Silvennoinen, R., Lehto, T., & Pelkonen, P. (2011). Analysis of the willow root system by electrical impedance spectroscopy. *Journal of Experimental Botany, 62*, 351–358.

Chi, M. L., Chen, L. H., & Chen, T. M. (2012). The development and application of an electrical impedance spectroscopy measurement system for plant tissues. *Computers and Electronics in Agriculture, 82*, 96–99.

Cole, K. S. (1932). Electric phase angle of cell membranes. *The Journal of General Physiology, 15*(6), 641–649.

Greenham, C. G., Randall, P. J., & Müller, W. J. (1982). Studies of phosphorus and potassium deficiencies in Trifolium subterraneum based on electrical measurements. *Canadian Journal of Botany, 60*, 634–644.

Hayden, R. I., Moyse, C. A., Calder, F. W., Crawford, D. P., & Fensom, D. S. (1969). Electrical impedance studies on potato and alfalfa tissue. *Journal of Experimental Botany, 20*, 177–200.

He, J. X., Wang, Z. Y., Shi, Y. L., Qin, Y., Zhao, D. J., & Huang, L. (2011). A prototype portable system for bioelectrical impedance spectroscopy. *Sensor Letters, 9*, 1151–1156.

Hinton, A. J., & Sayers, B. (1998). *Advanced instrumentation for bioimpedance measurements*. UK: Solartron Analytical.

Hsu, C. H., & Mansfeld, F. (2001). Concerning the conversion of the constant phase element parameter Y0 into a capacitance. *Corrosion, 57*, 747–748.

Itagaki, M., Taya, A., Watanabe, K., & Noda, K. (2002). Deviations of capacitive and inductive loops in the electrochemical impedance of a dissolving iron electrode. *Analytical Sciences, 18*, 641–644.

Jackson, P. J., & Harker, F. R. (2000). Apple bruise detection by electrical impedance measurement. *HortScience, 35*, 104–107.

Jorcin, J. B., Orazem, M. E., Pebere, N., & Tribollet, B. (2006). CPE analysis by local electrochemical impedance spectroscopy. *Electrochimica Acta, 51*, 1473–1479.

Juansah, J., Budiastra, I. W., Dahlan, K., & Boroseminar, K. (2012). The prospect of electrical impedance spectroscopy as non-destructive evaluation of citrus acidity. *International Journal of Emerging Technology and Advanced Engineering, 2*(11), 58–64.

Kumar, V., Singh, T. R., Hada, A., Jolly, M., Ganapathi, A., & Sachdev, A. (2015). Probing phosphorus efficient low phytic acid content soybean genotypes with phosphorus starvation in hydroponics growth system. *Applied Biochemistry and Biotechnology, 177*, 689–699.

Liu, X. (2006). *Electrical impedance spectroscopy applied in plant physiology studies* (M.Sc. thesis). Melbourne, Australia: RMIT University.

Macdonald, J. R. (1992). Impedance spectroscopy. *Annals of Biomedical Engineering, 20*, 289–305.

Mizukami, Y., Sawai, Y., & Yamaguchi, Y. (2006). Moisture content measurement of tea leaves by electrical impedance and capacitance. *Biosystems Engineering, 93*(3), 293–299.

Pethig, R., & Kell, D. B. (1987). The passive electrical properties of biological systems: their significance in physiology, biophysics and biotechnology. *Physics in Medicine and Biology, 32*, 933–970.

Rafael, F. M. H., Antonio, deJ. O. M., Ramon, G. G. G., Irineo, T. P., & Gilberto, H. R. (2014). An analysis of electrical impedance measurements applied for plant N status estimation in Lettuce (Lactuca sativa). *Sensors, 14*, 11492–11503.

Ricciardi, S., Ruiz-Morales, J. C., & Nunez, P. (2009). Origin and quantitative analysis of the constant phase element of a platinum SOFC cathode using the state-space model. *Solid State Ionics, 180*, 1083–1090.

Skale, S., Dolecek, V., & Slemnik, M. (2007). Substitution of the constant phase element by Warburg impedance for protective coatings. *Corrosion Science, 49*, 1045–1055.

Tomkiewicz, D., & Piskier, T. (2012). A plant based sensing method for nutrition stress monitoring. *Precision Agriculture, 13*, 370–383.

Wang, L., Bai, Y., & Lu. (2006). Research advance on plant nutrition diagnosis based on spectral theory (in Chinese). *Plant Nutrition and Fertilizer Science, 12*(60), 902–912.

Wu, L., Ogawa, Y., & Tagawa, A. (2008). Electrical impedance spectroscopy analysis of eggplant pulp and effects of drying and freezing-thawing treatments on its impedance characteristics. *Journal of Food Engineering, 87*, 274–280.

Yasumasa, A., Koichi, M., & Naoto, W. (2014). .Electrical impedance analysis of potato tissues during drying. *Journal of Food Engineering, 121*, 24–31.

Yu, W. G., & Zhao, T. M. (2005). *Tomato cultivation new technology*. Fujian: Fujian Science and Technology Press.

Zhang, M., Repo, T., Willison, J., & Sutinen, S. (1995). Electrical impedance analysis in plant tissues: on the biological meaning of Cole-Cole α in scots pine needles. *European Biophysics Journal, 24*, 99–106.

Zhang, M., & Willison, J. (1991). Electrical impedance analysis in plant tissues. *Journal of Experimental Botany, 42*, 1465–1475.

Zhang, M., & Willison, J. (1992). Electrical impedance analysis in plant tissues: the effect of freeze-thaw injury on the electrical

properties of potato tuber and carrot root tissues. *Canadian Journal of Plant Science, 72*, 545–553.
Zoltowski, P. (1998). On the electrical capacitance of interfaces exhibiting constant phase element behavior. *Journal of Electroanalytical Chemistry, 443*, 149–154.
Khaled El D., Castellano, N. N., Gazquez, J. A., García Salvador, R. M., & Manzano-Agugliaro, F. Cleaner quality control system using bioimpedance methods: a review for fruits and vegetables, Journal of Cleaner Production, Available online 10 November 2015, ISSN 0959-6526, http://dx.doi.org/10.1016/j.jclepro.2015.10.096.